Chapitre 1

A fully discrete scheme for diffusive-dispersive conservation laws

Ce chapitre a fait l'objet d'une publication dans le journal *Numerische Mathematik*: voir [24]

A fully discrete scheme for diffusive-dispersive conservation laws

C. Chalons[1] and P.G. LeFloch[2]

Résumé

We introduce a fully discrete (in both space and time) scheme for the numerical approximation of diffusive-dispersive hyperbolic conservation laws in one-space dimension. This scheme extends an approach by LeFloch and Rohde [94]: it satisfies a cell entropy inequality and, as a consequence, the space integral of the entropy is a decreasing function of time. This is an important stability property, shared by the continuous model as well. Following Hayes and LeFloch [64], we show that the limiting solutions generated by the scheme need not coincide with the classical Oleinik-Kruzkov entropy solutions, but contain nonclassical undercompressive shock waves. Investigating the properties of the scheme, we stress various similarities and differences between the continuous model and the discrete scheme (dynamics of nonclassical shocks, nucleation, etc).

1.1 Introduction

In this paper, we are interested in the numerical approximation of the *limiting* solutions generated by the diffusive-dispersive conservation law [87]:

$$\partial_t u + \partial_x f(u) = \epsilon\,\beta\, U'(u)_{xx} + \epsilon^2\,\gamma\, U'(u)_{xxx}, \qquad u = u_\epsilon^{\beta,\gamma}(x,t), \quad x \in I\!R,\ t > 0, \tag{1.1}$$

when $\epsilon > 0$ tends to zero. Here the flux $f : I\!R \to I\!R$ is a smooth given function and $\beta, \gamma > 0$ are fixed parameters. In the right-hand side of (1.1), $U : I\!R \to I\!R$ is a given, strictly convex function. The following is known concerning the limiting solutions $\lim_{\epsilon\to 0} u_\epsilon^{\beta,\gamma}$. (We refer to the review [87] and the references cited therein.) First of all, they generally depend on the parameters β and γ. Based on simple scaling arguments, one can see that they only depend on the ratio $\delta = \beta/\gamma$. So we define

$$u^\delta := \lim_{\epsilon\to 0} u_\epsilon^{\beta,\gamma}, \tag{1.2}$$

provided the limit exists in some strong topology. Based on (1.1) and

$$\begin{aligned}\partial_t U(u) + \partial_x F(u) \;&=\; \tfrac{\epsilon\beta}{2}\,(U'(u)^2)_x \\ &-\; \epsilon\,\beta\, U'(u)_x^2 + \epsilon^2\gamma\, \left(U'(u)\, U'(u)_{xx} - U'(u)_x^2/2\right)_x,\end{aligned}$$

it is easy to check that the function u^δ satisfies the hyperbolic conservation law

$$\partial_t u + \partial_x f(u) = 0, \tag{1.3}$$

1. O.N.E.R.A., B.P. 72, 29 avenue de la Division Leclerc, 92322 Châtillon Cedex, France. E-mail address: chalons@onera.fr.

2. Centre de Mathématiques Appliquées & Centre National de la Recherche Scientifique, U.M.R. 7641, Ecole Polytechnique, 91128 Palaiseau Cedex, France. E-mail address: lefloch@cmap.polytechnique.fr.

and the entropy inequality

$$\partial_t U(u) + \partial_x F(u) \le 0, \tag{1.4}$$

where U is regarded as an "entropy" of (1.3), and $F : I\!R \to I\!R$ is the corresponding entropy flux defined by $F'(u) = U'(u)\, f'(u)$. Note also that from (1.4) it follows that

$$\int_{I\!R} U(u(x,t))\, dx \le \int_{I\!R} U(u(x,s))\, dx, \qquad t \ge s. \tag{1.5}$$

In this paper, we propose a fully discrete (in space and time) finite difference scheme for the numerical approximation of the solutions u^δ in (1.2). We rely on the approach developed recently by LeFloch and Rohde [94] and based on Tadmor's notion of entropy conservative flux (see [134]) for the hyperbolic part of (1.1). We will introduce here a fully discrete version of the semi-discrete scheme derived in [94]. The high-order accuracy in time is provided by a standard Runge-Kutta technique. In Section 1.2, we can prove that our fully discrete scheme satisfies a cell entropy inequality, which implies that the entropy is a decreasing function of time. See Theorem 13 and Corollary 8.

In Section 1.3, we investigate the properties of our scheme, especially in terms of stability and nucleation. The stability condition derived in Section 1.2 is numerically investigated. We also demonstrate that the scheme admits a nucleation threshold. Above the threshold value, nonclassical solutions violating the standard entropy criterion are observed. The dependence of the threshold in δ is investigated. We recall that these undercompressive, nonclassical solutions play an important role in many models of continum mechanics when diffusive and dispersive effects are in balance [87].

1.2 A fully discrete scheme

We start from the semi-discrete method derived by LeFloch and Rohde [94]. Consider the following scheme in conservative form (j describing the integers)

$$\frac{d}{dt} u_j(t) = -\frac{1}{h}\left(g_{j+1/2}(t) - g_{j-1/2}(t)\right), \qquad t \ge 0, \tag{1.6}$$

with $g_{j+1/2}(t) := g(u_{j-1}(t), u_j(t), u_{j+1}(t), u_{j+2}(t))$, the parameter $h > 0$ being the mesh size. The numerical flux has the form $g := g^1 + g^2 + g^3$, where g^1 is consistent with the hyperbolic flux $f(u)$, g^2 is an approximation of $\beta\, h\, U'(u)_x$, and g^2 of $\gamma\, h^2\, U'(u)_{xx}$. More precisely, using the entropy variable

$$v := U'(u), \quad g(v) := f(u), \quad G(v) := F(u),$$

and therefore $v_0 := U'(u_0)$, etc, we define

$$g^1(u_{-1}, u_0, u_1, , u_2) := \int_0^1 g(v_0 + s(v_1 - v_0))\, ds - \frac{1}{12}(v_2 - v_1 - v_0 + v_{-1}) g'(v_0), \tag{1.7}$$

$$g^2(v_0, v_1) := -\frac{\beta}{2}\,(v_1 - v_0), \tag{1.8}$$

and

$$g^3(v_{-1}, v_0, v_1, v_2) := -\frac{\gamma}{6}\,(v_2 - v_1 - v_0 + v_{-1}). \tag{1.9}$$

Note that we are using the *same* notation for the exact flux $g = g(v)$ expressed in the entropy variable and for the numerical flux.

Theorem 11
The scheme (1.6)-(1.7)-(1.8)-(1.9) is conservatif and consistent with the hyperbolic conservation law (1.3). It also satisfies the cell entropy inequality ($t \geq 0$ and j describing the integers)

$$\frac{d}{dt}U(u_j(t)) + \frac{1}{h}\left(G_{j+1/2}(t) - G_{j-1/2}(t)\right) \leq 0, \tag{1.10}$$

where the numerical entropy flux has the form $G := G^1 + G^2 + G^3$, where

$$\begin{aligned} G^1(v_{-1}, v_0, v_1, v_2) \; &:= \; \tfrac{(v_0+v_1)}{2} g(v_{-1}, v_0, v_1, v_2) \\ &- \; \tfrac{1}{2}\Big(\psi(v_0, v_1, v_2) + \psi(v_{-1}, v_0, v_1)\Big) \end{aligned} \tag{1.11}$$

with

$$\psi(v_0, v_1, v_2) := v_1 g(v_1) - G(v_1) + \frac{1}{12}(v_1 - v_0) g'(v_0)\,(v_1 - v_2),$$

$$G^2(v_0, v_1) := -\frac{\beta}{4}\left(v_1^2 - v_0^2\right), \tag{1.12}$$

and

$$G^3(v_{-1}, v_0, v_1, v_2) = -\frac{\gamma}{6}\Big(v_{-1}v_1 + v_0 v_2 - 2\, v_0 v_1\Big). \tag{1.13}$$

Moreover, the equivalent equation of the scheme (1.6)-(1.7)-(1.8)-(1.9), up to the (third-order) terms in h^2, coincide with the continuous model (1.1) provided ϵ is replaced with h.

Proof
It is straightforward to calculate that

$$\frac{d}{dt}U(u_j(t)) + \frac{1}{h}\Big(G_{j+1/2}(t) - G_{j-1/2}(t)\Big) = -D_j(t), \tag{1.14}$$

where

$$D_j(t) = \frac{\beta}{4}\left(|v_j(t) - v_{j-1}(t)|^2 + |v_{j+1}(t) - v_j(t)|^2\right) \geq 0.$$

The second claim in the theorem follows by performing a Taylor expansion in (1.6) and by using the definitions (1.7)-(1.8)-(1.9). □

We now turn to defining our fully discrete scheme, having in mind to generalize Theorem 11, under some CFL stability restriction on the time discretization. To begin with, we analyze a first order time-discretization. Denote by $k > 0$ the size of the regularly spaced time-mesh. Consider the following scheme ($n \geq 0$ and j describing the integers)

$$u_j^{n+1} = u_j^n - \lambda\,(g_{j+1/2}^n - g_{j-1/2}^n), \tag{1.15}$$

where the ratio $\lambda = k/h$ is kept fixed. In (1.15), we use the notation $g_{j+1/2}^n := g(u_{j-1}^n, u_j^n, u_{j+1}^n, u_{j+2}^n)$, and we define $G_{j+1/2}^n$ similarly, etc.

Theorem 12
The scheme (1.15) satisfies the cell entropy inequality

$$\begin{aligned} & U(u_j^{n+1}) - U(u_j^n) + \lambda\,(G_{j+1/2}^n - G_{j-1/2}^n) + \tfrac{\beta\,\lambda}{4}\,(|v_j^n - v_{j-1}^n|^2 + |v_{j+1}^n - v_j^n|^2) \\ & \le 3\lambda^2\,\|U''\|_\infty\,(\|g'\|_\infty^2\,D_j^{1,n} + \beta^2\,D_j^{2,n} + \gamma^2\,D_j^{3,n}), \end{aligned} \tag{1.16}$$

where

$$D_j^{1,n} := \frac{1}{36}\,(|v_{j-1}^n - v_{j-2}^n|^2 + 73\,|v_j^n - v_{j-1}^n|^2 + 73\,|v_{j+1}^n - v_j^n|^2 + |v_{j+2}^n - v_{j+1}^n|^2),$$

$$D_j^{2,n} := \frac{1}{4}\,(|v_j^n - v_{j-1}^n|^2 + |v_{j+1}^n - v_j^n|^2),$$

and

$$D_j^{3,n} := \frac{1}{18}\,(|v_{j-1}^n - v_{j-2}^n|^2 + |v_j^n - v_{j-1}^n|^2 + |v_{j+1}^n - v_j^n|^2 + |v_{j+2}^n - v_{j+1}^n|^2).$$

Hence, for λ sufficiently small, the entropy is a strictly decreasing function of time, in the sense

$$\sum_{j=-\infty}^{\infty} U(u_j^{n+1}) + K\,\lambda \sum_{j=-\infty}^{\infty} |v_j^n - v_{j-1}^n|^2 \le \sum_{j=-\infty}^{\infty} U(u_j^n), \tag{1.17}$$

with

$$K := \frac{\beta}{2} - 3\lambda\,\|U''\|_\infty\,(\frac{37}{9}\,\|g'\|_\infty^2 + \frac{\beta^2}{2} + \frac{2}{9}\,\gamma^2).$$

Furthermore, for smooth solutions, the equivalent equation of the scheme (1.15) is

$$\partial_t u + \partial_x f(u) = h\,\beta\,U'(u)_{xx} + h^2\,\gamma\,U'(u)_{xxx} + O(h^3 + k). \tag{1.18}$$

Observe that the equation (1.18) no longer correspond to the continous model (1.1). Namely the time-discretization generates a term of order $O(k)$ which can not be absorbed in the cubic error $O(h^3)$ (except of course if we were to impose the very drastic restriction $k = O(h^3)$.) Therefore a more accurate time-discretization will be necessary.

Proof
By a Taylor expansion in λ we can deduce from (1.15) that

$$U(u_j^{n+1}) - U(u_j^n) + \lambda\,U'(u_j^n)\,(g_{j+1/2}^n - g_{j-1/2}^n) \le \frac{\lambda^2}{2}\,\|U''\|_\infty\,|g_{j+1/2}^n - g_{j-1/2}^n|^2. \tag{1.19}$$

We determine the right hand side of (1.19) by treating successively the terms in

$$\begin{aligned} \tfrac{1}{2}\,|g_{j+1/2}^n - g_{j-1/2}^n|^2 \quad & \le \quad 3(|g_{j+1/2}^n - g(v_j^n)|^2 + |g(v_j^n) - g_{j-1/2}^n|^2 \\ & + \quad |g_{j+1/2}^{2,n}|^2 + |g_{j-1/2}^{2,n}|^2 + |g_{j+1/2}^{3,n}|^2 + |g_{j-1/2}^{3,n}|^2). \end{aligned}$$

In view of (1.7)-(1.8)-(1.9) we find

$$\frac{1}{2}\,|g_{j+1/2}^n - g(v_j^n)|^2 \le \|Dg\|_\infty^2\,(\frac{1}{72}\,|v_j - v_{j-1}|^2 + |v_{j+1} - v_j|^2 + \frac{1}{72}\,|v_{j+2} - v_{j+1}|^2),$$

and the same inequality remains true by replacing $g(v_j^n)$ with $g(v_{j+1}^n)$. On the other hand,

$$|g_{j+1/2}^{2,n}|^2 + |g_{j-1/2}^{2,n}|^2 \le \frac{\beta^2}{4}\,(|v_j - v_{j-1}|^2 + |v_{j+1} - v_j|^2),$$

$$|g_{j+1/2}^{3,n}|^2 + |g_{j-1/2}^{3,n}|^2 \le$$

$$\tfrac{\gamma^2}{18}\,(|v_{j-1} - v_{j-2}|^2 + |v_j - v_{j-1}|^2 + |v_{j+1} - v_j|^2 + |v_{j+2} - v_{j+1}|^2).$$

The desired inequality (1.16) then follows. Finally, summing over all value j and shifting the index $j \mapsto j+1$ or $j \mapsto j-1$ whenever necessary, one deduce (1.17) from (1.16).

The statement about the order of accuracy of the scheme is an immediate consequence of the corresponding properties known for the semi-discrete scheme; see Theorem 11. □

In view of (1.17), the entropy is a decreasing function of time provided K is positive. This leads us to the following CFL-like restriction on λ to ensure the stability of the scheme:

$$6\,\lambda\,\frac{\|U''\|_\infty}{\beta}\,(\frac{37}{9}\,\|g'\|_\infty^2 + \frac{\beta^2}{2} + \frac{2}{9}\,\gamma^2) \le 1. \tag{1.20}$$

Of course, (1.20) also depends on β, γ and the maximum speed $\|g'\|_\infty$, as well as the entropy U.

It is interesting to observe that, in the limit $\lambda \to 0$, that is $k \to 0$ but h kept fixed, the entropy inequality (1.16) implies the semi-discrete one, (1.10), while (1.17) tends to (namely, $K \to \beta/2$)

$$\frac{d}{dt}\sum_{j=-\infty}^{\infty} U(u_j) + \frac{\beta}{2}\sum_{j=-\infty}^{\infty} |v_j(t) - v_{j-1}(t)|^2 \le 0. \tag{1.21}$$

We stress that the stability condition (1.20) is trivially satisfied in the limit $\lambda \to 0$! Indeed, the semi-discrete scheme (1.6)-(1.7)-(1.8)-(1.9) is unconditionnally stable (in the sense that (1.10)-(1.11)-(1.12)-(1.13) holds).

To obtain, as in LeFloch and Rohde [94], a scheme whose equivalent equation coincides with (1.1), we need to increase the order of discretization in time, to the third order, at least. Following Shu [121], we rely on a Runge-Kutta technique. Observe that the (first order in time) scheme can be rewritten in the form

$$\begin{aligned} &(i) \qquad u_j^{n+1} = u_j^n + L(u^n)_j, \\ &(ii) \qquad L(u^n)_j = -\lambda\,(g_{j+1/2}^n - g_{j-1/2}^n). \end{aligned} \tag{1.22}$$

A high-order accurate (in time) scheme is obtained by the Runge-Kutta technique, as follows:

$$\begin{aligned} &(i) \qquad u_j^{n+1} = \textstyle\sum_{k=0}^m (\alpha_k\,u_j^{n-k} + \beta_k\,L(u^{n-k})_j), \\ &(ii) \qquad u_j^{-k} = u_j^0, \quad k = 0, 1, ..., m. \end{aligned} \tag{1.23}$$

In the above, the coefficients α_k and β_k can be determined to have third-order accuracy in time. In our numerical experiments below, we will use

$$\begin{aligned} &m = 3, \\ &\alpha_0 = \tfrac{16}{27}\,,\ \alpha_1 = \alpha_2 = 0\,,\ \alpha_3 = \tfrac{11}{27}, \\ &\beta_0 = \tfrac{16}{9}\,,\ \beta_1 = \beta_2 = 0\,,\ \beta_3 = \tfrac{44}{27}, \end{aligned} \tag{1.24}$$

Note that the coefficients are positive and of unit sum, i.e.,

$$\begin{aligned} &\alpha_k \geq 0, \qquad k = 0, 1, ..., m, \\ &\textstyle\sum_{k=0}^m \alpha_k = 1. \end{aligned} \tag{1.25}$$

Theorem 13
Assume that the coefficients α_k, $k = 0, \dots, m$, satisfy the condition (1.25). Then the fully discrete scheme (1.23) satisfies the following local entropy inequality

$$\begin{aligned} &U(u_j^{n+1}) - \textstyle\sum_{k=0}^m \alpha_k U(u_j^{n-k}) + \lambda \sum_{k=0}^m \beta_k (G_{j+1/2}^{n-k} - G_{j-1/2}^{n-k}) \\ &+\tfrac{\lambda\beta}{4} \textstyle\sum_{k=0}^m \beta_k \left(|v_{j+1}^{n-k} - v_j^{n-k}|^2 + |v_j^{n-k} - v_{j-1}^{n-k}|^2\right) \\ &\leq \lambda^2 \textstyle\sum_{k=0}^m \frac{3\,\beta_k^2}{\alpha_k} \|U''\|_\infty \left(\|g'\|_\infty^2\, D_j^{1,n-k} + \beta^2\, D_j^{2,n-k} + \gamma^2\, D_j^{3,n-k}\right). \end{aligned} \tag{1.26}$$

Hence, the entropy satisfies

$$\sum_{j=-\infty}^{+\infty} U(u_j^{n+1}) + \lambda \sum_{j=-\infty}^{+\infty} \sum_{k=0}^{m} d_k\, |v_{j+1}^{n-k} - v_j^{n-k}|^2 \leq \sum_{j=-\infty}^{+\infty} \sum_{k=0}^{m} \alpha_k U(u_j^{n-k}), \tag{1.27}$$

where

$$d_k := \frac{\beta\,\beta_k}{2} - \frac{3\,\lambda\,\beta_k^2}{\alpha_k} \|U''\|_\infty \left(\|g'\|_\infty^2 \frac{37}{9} + \frac{\beta^2}{2} + \frac{2\gamma^2}{9}\right), \tag{1.28}$$

with the convention that $\beta_k/\alpha_k = 0$ when $\alpha_k = \beta_k = 0$. If the coefficients are chosen as in (1.24), then the equivalent equation of the scheme (1.23) is

$$\partial_t u + \partial_x f(u) = h\,\beta\, U'(u)_{xx} + h^2\,\gamma\, U'(u)_{xxx} + O(h^3 + k^3), \tag{1.29}$$

which, up to quadratic terms in h, coincides with the continuous model (1.1) provided h is replaced with ϵ.

Proof
In view of (1.25), the scheme (1.23i) admits the following convex decomposition:

$$u_j^{n+1} = \sum_{k=0}^{m} \alpha_k\, w_j^{n-k}, \tag{1.30}$$

with

$$w_j^{n-k} = u_j^{n-k} + \frac{\lambda\,\beta_k}{\alpha_k}\, L(u^{n-k})_j. \tag{1.31}$$

Since the entropy U is a convex function, we deduce from (1.30) that

$$U(u_j^{n+1}) \leq \sum_{k=0}^{m} \alpha_k \, U(w_j^{n-k}).$$

Therefore, using the entropy inequality (1.16) with λ replaced with $\lambda\,\beta_k/\alpha_k$, we obtain immediately the inequality (1.26).

The global entropy inequality (1.27) is a consequence of (1.26), obtained by summing over all j and then shifting the index whenever needed. □

In view of (1.28), it is natural to impose the following CFL-like *stability restriction* on the ratio $\lambda = k/h$:

$$\begin{aligned} &(i) && 6\,\lambda\,\sup_{0\leq k\leq m} \tfrac{\beta_k}{\alpha_k}\,\tfrac{\|U''\|_\infty}{\beta}\left(\|g'\|_\infty^2\,\tfrac{37}{9}+\tfrac{\beta^2}{2}+\tfrac{2\,\gamma^2}{9}\right)\leq 1,\\ &(ii) && \beta_k \geq 0. \end{aligned} \tag{1.32}$$

At this juncture, recall that the limiting solution $\lim_{\epsilon\to 0} u_\epsilon^{\beta,\gamma}$ only depends on the ratio $\delta = \beta/\gamma$. So, for a given value of δ, it is natural to choose β so that to minimize the constrain in (1.32), i.e. to minimize

$$\frac{\beta_k}{\alpha_k}\,\frac{\|U''\|_\infty}{\beta}\left(\|g'\|_\infty^2\,\frac{37}{9}+\frac{\beta^2}{2}+\frac{2\,\beta^2}{9\,\delta^2}\right),$$

with respect to all $\beta > 0$. It is easy to check that we can then replace (1.32) with

$$\begin{aligned} &(i) && 12\,\lambda\,\sup_{0\leq k\leq m} \tfrac{\beta_k}{\alpha_k}\,\|U''\|_\infty\left(\|g'\|_\infty^2\,\tfrac{37}{9}\left(\tfrac{1}{2}+\tfrac{2}{9\,\delta^2}\right)\right)^{1/2}\leq 1,\\ &(ii) && \beta_k \geq 0. \end{aligned} \tag{1.33}$$

From Theorem 13 we deduce that the entropy can never exceed the entropy at time $t = 0$.

Corollary 8
Under the restriction (1.32), we have

$$\sum_{j=-\infty}^{\infty} U(u_j^n) \leq \sum_{j=-\infty}^{\infty} U(u_j^0). \tag{1.34}$$

Proof
In view of (1.32), the coefficients in (1.28) are positive, so that (1.27) gives us

$$\sum_{j=-\infty}^{+\infty} U(u_j^{n+1}) \leq \sum_{j=-\infty}^{+\infty}\sum_{k=0}^{m} \alpha_k\, U(u_j^{n-k}). \tag{1.35}$$

We then proceed by induction on n. When $n = 0$, the inequality (1.35) together with (1.23ii) yields exactly

$$\sum_{j=-\infty}^{\infty} U(u_j^1) \leq \sum_{j=-\infty}^{\infty} U(u_j^0),$$

which is (1.34).

If now, for some N,

$$\sum_{j=-\infty}^{\infty} U(u_j^n) \leq \sum_{j=-\infty}^{\infty} U(u_j^0) \qquad \text{for all } n \leq N,$$

then it follows again from (1.35) and (1.23ii) that

$$\sum_{j=-\infty}^{\infty} U(u_j^{N+1}) \leq \sum_{j=-\infty}^{+\infty} \sum_{k=0}^{m} \alpha_k U(u_j^0) = \sum_{j=-\infty}^{\infty} U(u_j^0).$$

This completes the proof of (1.34). □

It is clear that, if the solution is periodic in space, then the inequality (1.27) still holds when we sum up over one period. Thus (1.34) also holds true on one period. This observation will be used in next section, where we will numerically test the validity of this inequality.

1.3 Numerical experiments

In the present section, following Hayes and LeFloch [64], we experiment with the scheme proposed in Section 1.2. We demonstrate now that, in the limit $h \to 0$ (with $\lambda = k/h$ kept fixed), our fully discrete scheme generates nonclassical shock waves. We also check the monotonicity of the entropy as a function of time, in agreement with Corollary 8. On the other hand, we investigate the nucleation property of the scheme by studying the Riemann problem. In particular, we observe that, when the Riemann data remain below some threshold value, the corresponding solutions are always classical. All these properties were also met with the continuous model (1.1); see [87] and the references therein.

Let us recall that finite difference schemes for scalar conservation laws with nonconvex flux may contain some oscillations and, as a consequence, converge to (nonmonotone) nonclassical solutions. See LeFloch [87] for a review. Such a behavior can be avoided by restricting attention to TVD (total variation diminishing) schemes (after Harten). Indeed, in a TVD scheme, the number of local maxima or minima is a decreasing function of time, and as was observed in [69], such a scheme can not generate nonclassical shocks. The TVD approach is not applicable to handle limiting solutions generated by the diffusive-dispersive model (1.1), since the (nonclassical) solutions of interest do not possess monotonicity properties in general.

All the numerical experiments in this section will be done with the model (1.1) and the following choice of flux and entropy:

$$f(u) = u^3 - u, \quad U(u) = u^2/2, \qquad u \in I\!R. \tag{1.36}$$

The coefficients α_k and β_k given by (1.24) will be used. The time step is always taken to be the largest allowed by our CFL stability condition (1.32), excepted when it is mentionned otherwise. The space variable is taken to be $x \in [-1/2, 1/2]$.

Experiments 1 : We start by displaying some typical solutions generated by our scheme. The physical and numerical coefficients are chosen to be $\beta = 5.0$ and $\gamma = 37.5$

. We used 800 mesh points and t is equal to 0.003 and multiplied the condition (1.32) by a factor 20.

In Figure 1.1, we present, after about 8000 iterations of time, a two-wave solution, made of a nonclassical shock preceeded by a classical shock. Observe that the solution is non-monotone, altough it has been generated from a monotone Riemann data:

$$u(x,0) = \begin{cases} u_l & \text{for } x < 0, \\ u_r & \text{for } x > 0. \end{cases} \tag{1.37}$$

Here we have used $u_l = 4$ and $u_r = -3$.

In Figure 1.2, we display a two-wave solution containing a nonclassical shock and a rarefaction wave. Observe that the two waves are not attached, as it would be in a solution containing classical shocks only. Here we have $u_l = 4$ and $u_r = -3$ and about 15000 iterations of time have been used.

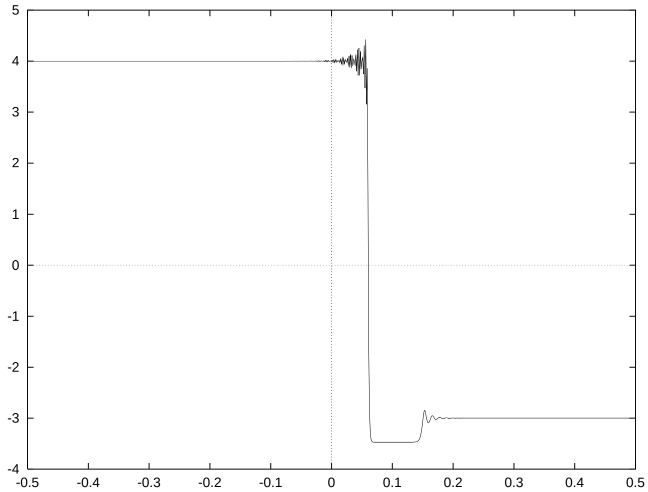

FIG. 1.1 – *A nonclassical shock + a classical shock*

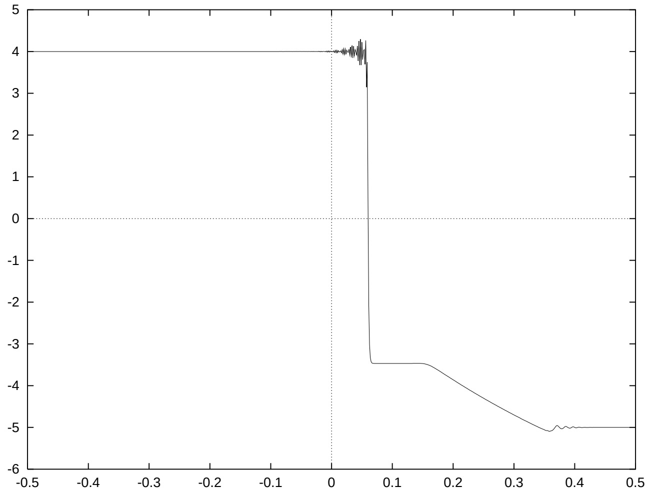

FIG. 1.2 – *A nonclassical shock + a rarefaction*

Experiments 2 : We want now to test the stability condition (1.32) on λ, found analytically in Section 1.2. First of all we demonstrate that the entropy is decreasing in time. Consider the periodic initial data $u(x,0) = -\sin(2\pi x))$ for $x \in [-1/2, 1/2]$ and let us solve (1.1) with periodic boundary conditions. The following parameters will be used

$$h = 0.00125, \qquad \beta = 5.0, \qquad \gamma = 18.75.$$

We want to test the validity of (1.34) on one period. The large-time behavior of the solution is displayed in Figure 1.3. We used here about 48000 iterations (with (1.33) as CFL-like condition) in time to reach the time $t = 0.24$. The solution contains a nonclassical shock and a rarefaction wave.

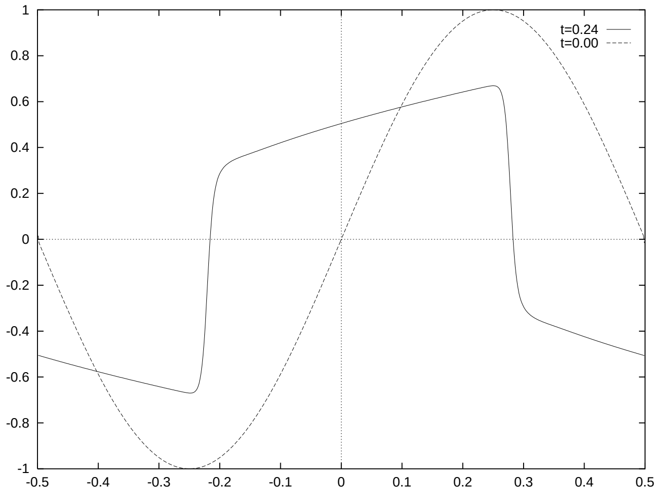

FIG. 1.3 – *A nonclassical shock + a rarefaction*

For λ sufficiently small, we observe that the decrease predicted by Corollary 8 holds. See Figure 1.4.

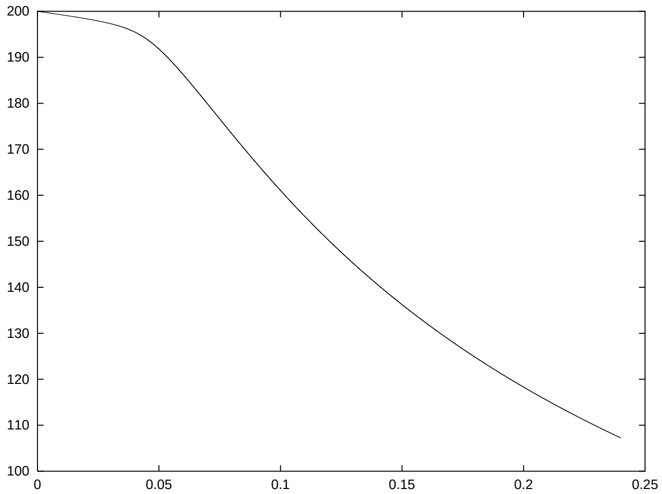

FIG. 1.4 – *Entropy versus time*

However, increasing λ, we note that, while the scheme still converges to nonclassical solutions (having oscillations of larger amplitude, however), it may well increase the entropy. For example, multiplying the time-step (1.32) by a factor 12, we see on Figures 1.5 and 1.6 that, even for small times, the scheme is less stable and the solutions much oscillatory, and (1.34) is violated. In fact, even the local in time inequality (1.27) is violated. However, the entropy remains decreasing in average.

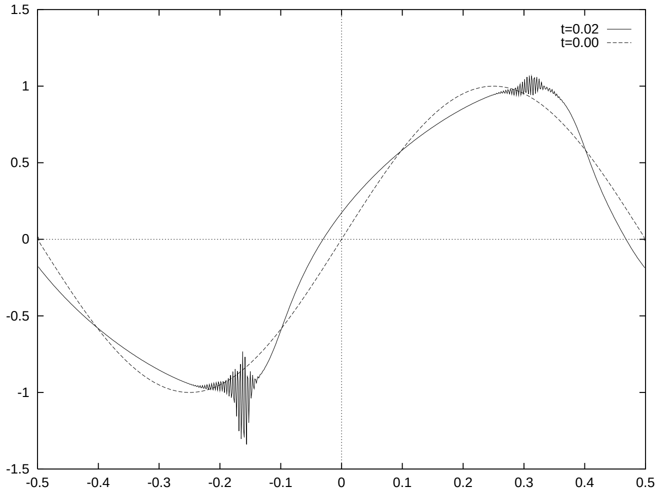

FIG. 1.5 – *Numerical solution with a large CFL*

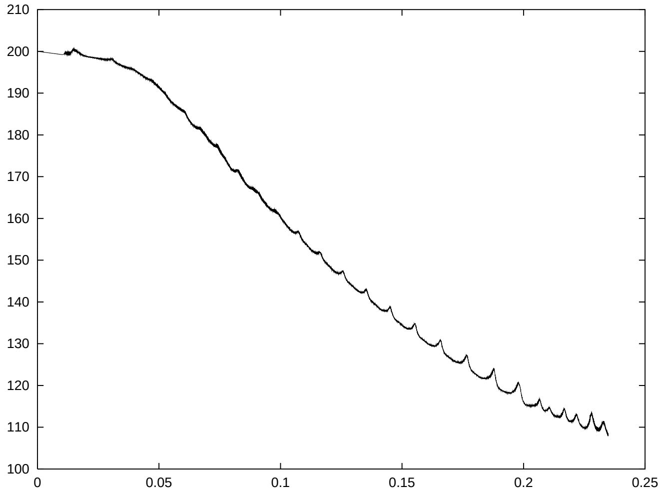

FIG. 1.6 – *Entropy with a large CFL*

Finally, our numerical tests demonstrate that the entropy may well increase when the conditions of the theorems in Section 1.2 are not fullfiled. Thereore the condition (1.32) on λ plays the role of a CFL condition, in a situation where one can not rely on the standard CFL condition (restricting λ in terms of the largest speed $|f'(u)|$ in the problem). Precisely, Figures 1.7 and 1.8 display some numerical solution obtained with our scheme but using now the standard CFL condition. Numerical oscillations are now much more important, and again (1.34) is violated. The time oscillations in Figure 1.8 have significantly larger amplitude than the ones in Figure 1.6. However, it would be interesting to derive further conditions on λ ensuring the stability of the scheme for arbitrary values of the parameters β and γ, precisely like the standard

CFL.

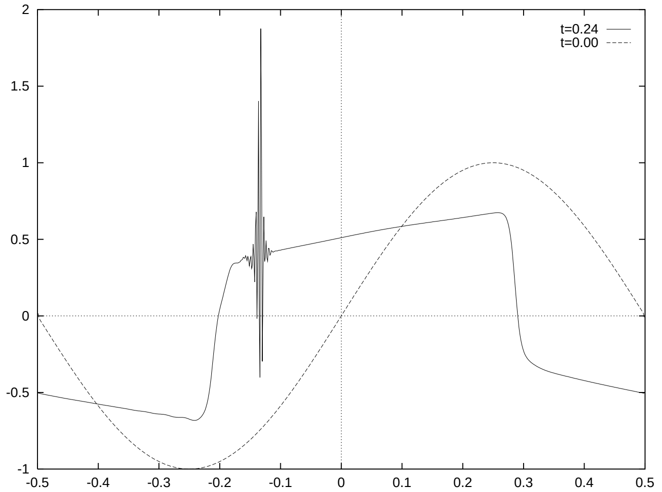

FIG. 1.7 – *Numerical solution with the standard CFL*

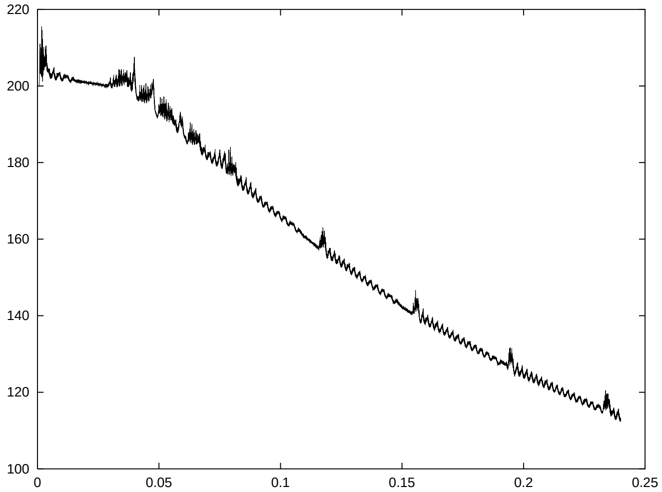

FIG. 1.8 – *Entropy with the standard CFL*

Experiments 3 : We now study how the scheme happens to nucleate nonclassical shocks. The discussion depends on the values on the Riemann data and the ratio of the diffusion to the dispersion. Consider the Riemann data (1.37) with $u_l > 0$ and $u_r < 0$. Motivated by a property of the continuous model (1.1), we claim that there exists a threshold $\psi(\delta)$ such that, for all $u_l < \psi(\delta)$, the Riemnann solution remains completely classical for arbitrary u_r, while for $u_l > \psi(\delta)$ the solution is nonclassical. This is indeed illustated by Figure 1.9, where

$$u_r = -5, \quad \beta = 5 \quad \text{and} \quad \gamma = 37.5.$$

The solution is classical when $u_l = 1$, but nonclassical when $u_l = 3$ or $u_l = 2$. The mesh contains 800 points for the cases $u_l = 3$ and $u_l = 4$, and 1200 points for the case $u_l = 1$. The numerical solutions are displayed at the time $t = 0.003$.

Similarly, there exists a threshold $\phi(u_l)$ such that, for $\delta > \psi(u_l)$, the Riemnann solution remains completely classical for arbitrary u_r, while for $\delta < \psi(u_l)$ the solution is always nonclassical. This is illustated in Figure 1.10, where

$$u_l = 4, \quad u_r = -5, \quad t = 0.003.$$

The solution is classical when $\beta = 30$, but nonclassical when $\beta = 5$ or $\beta = 15$. We used a grid made of 400 points and reduced δ by keeping γ fixed but by decreasing β.

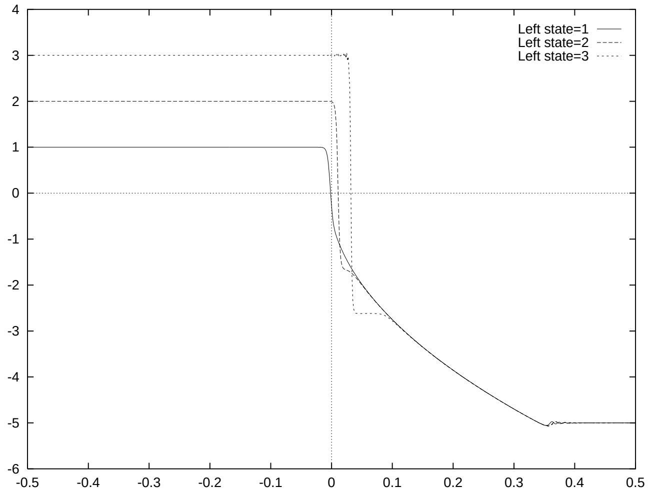

FIG. 1.9 – *Several values of u_l.*

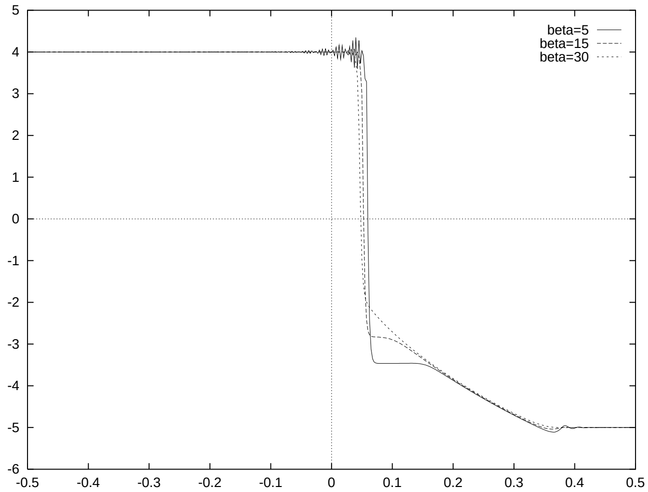

FIG. 1.10 – *Several values of β*

Finally, we claim that the function $\psi(\delta)$ increases when δ increases. To illustrate this point numerically, we consider the following parameters:

$$u_l = 4, \quad u_r = -5, \quad t = 0.003, \quad \beta = 5.$$

We used a mesh made of 800 points, and $\gamma = 1.75$, so that the ratio δ is larger, compared with the test in Figure 1.2. On Figure 1.11, the solution is classical.

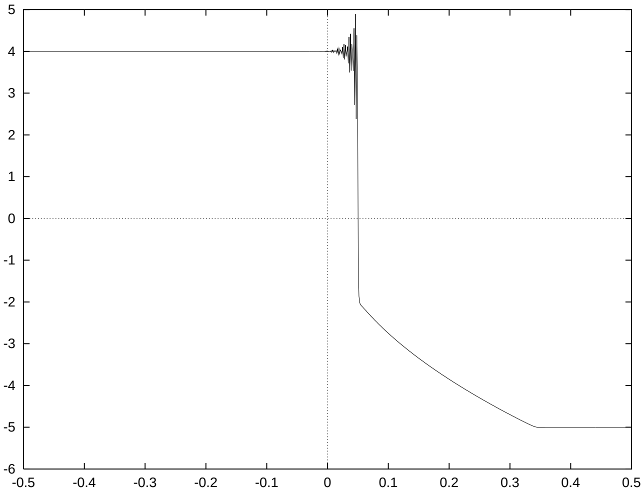

FIG. 1.11 – *Numerical solution for* $\gamma = 1.75$

Compare it with Figure 1.2 which has a nonclassical solution. This illustrates that $\psi(\delta)$ as δ increases.

1.4 Conclusion

To conclude, we emphasize that all the fundamental properties of the continuous model (1.1) are also shared by our numerical scheme. We demonstrated that the limiting solutions may contain undercompressive, nonclassical shocks that depend on the ratio δ. This happens only when the ratio of the diffusion to the dispersion is sufficiently small, or when the amplitude of the solution is sufficiently large. The class of schemes presented in this paper is efficient to compute nonclassical shock waves. For sufficiently small CFL numbers, the schemes satisfy exactly a discrete version of the entropy decay property (1.5); see Figure 1.4. Under a standard CFL condition, mild oscillations are observed in Figure 1.6, while the convergence toward the nonclassical solutions is still ensured.

Finally, we point out that the scheme proposed in Section 1.2 also applies to systems of conservation laws, and that for systems the entropy inequalities in Theorem 13 still hold.